3

Visualizing Calcium Signaling in Cells by Digitized Wide-Field and Confocal Fluorescent Microscopy

Michael Wm. Roe, Jerome F. Fiekers, Louis H. Philipson, and Vytautas P. Bindokas

Summary

Calcium (Ca^{2+}) is a fundamentally important component of cellular signal transduction. Dynamic changes in the concentration of Ca^{2+} ($[Ca^{2+}]$) in the cytoplasm and within organelles are tightly controlled and regulate a diverse array of biological activities, including fertilization, cell division, gene expression, cellular metabolism, protein biosynthesis, secretion, muscle contraction, intercellular communication, and cell death. Measurement of intracellular $[Ca^{2+}]$ is essential to understanding the role of Ca^{2+} and for defining the underlying regulatory mechanisms in any cellular process. A broad range of synthetic and biosynthetic fluorescent Ca^{2+} sensors are available that enable the visualization and quantification of subcellular spatio-temporal $[Ca^{2+}]$ gradients. This chapter describes the application of wide-field digitized video fluorescence microfluorometry and confocal microscopy to quantitatively image Ca^{2+} in cells with high temporal and spatial resolution.

Key Words: Intracellular calcium; signal transduction; cellular imaging; fluorescence; confocal microscopy; Fura-2; Fluo-3; cameleon; pericam; biosensor; transfection.

1. Introduction

Calcium is an essential second-messenger signal in all cell types. Many cellular processes, including mitosis, gene transcription, protein biosynthesis and processing, energy metabolism, membrane electrical activity, exocytosis, motility, receptor-mediated signal transduction, and intercellular communication, are regulated by highly coordinated, spatio-temporal gradients of the concentration of intracellular Ca^{2+} ($[Ca^{2+}]_i$), which can be transient, sustained, and oscillatory. Ca^{2+} homeostasis and signal transduction are precisely controlled by transport mechanisms and Ca^{2+}-binding proteins. Crucial to the regulation of Ca^{2+} signaling are mechanisms that control Ca^{2+} fluxes in the plasma membrane, endoplasmic reticulum, mitochondria, and Golgi complex.

From: *Methods in Molecular Biology, vol. 319: Cell Imaging Techniques: Methods and Protocols*
Edited by: D. J. Taatjes and B. T. Mossman © Humana Press Inc., Totowa, NJ

Understanding the role of Ca^{2+} in cell physiology and elucidation of the underlying regulatory mechanisms requires measurements of $[Ca^{2+}]_i$. In recent years, new technical developments in microscopy, digital cameras, and Ca^{2+} indicators have made the study of high-resolution, rapid changes in subcellular $[Ca^{2+}]$ possible. In this chapter, we describe the methods we employ to visualize Ca^{2+} signals in the cytoplasm and within organelles of electrically excitable endocrine cells in vitro.

Since the early 1980s, fluorescent synthetic Ca^{2+} dyes have been the most frequently used indicators to detect and visualize spatio-temporal $[Ca^{2+}]$ gradients in the cytoplasm and organelles of mammalian cells. Commercially available synthetic indicators such as Fura-2, Fluo-3, MagFura-2, and Rhod-2 can be easily loaded into cell suspensions and attached cells. The biophysical properties of synthetic fluorescent Ca^{2+} indicators are summarized in **Table 1**.

The general procedure for loading cells with a synthetic Ca^{2+} indicator involves incubation of cells in culture medium or physiological buffer that contains a membrane-permeable, acetoxymethyl ester (AM) precursor of the dye. Cellular nonspecific esterase activity facilitates removal of the ester and unmasks the negatively charged Ca^{2+}-binding site of the indicator. Consequently, the Ca^{2+}-sensitive anionic dye is trapped within the cytoplasm. This procedure, originally described by Tsien and his colleagues ***(1–5)***, allows labeling of large populations of cells with fluorescent Ca^{2+} indicators. However, because the lipophilic derivative of the indicator can partition across any membrane-surrounded organelle, it is extremely difficult to control the compartmentalization of the dye. This problem has long been recognized and methods for optimizing and evaluating dye loading conditions involving the evaluation of the effects of incubation time, temperature, and dye precursor concentration are described in detail elsewhere ***(6,7)***.

Notwithstanding these refinements, employing lipophilic precursors to load Ca^{2+} dyes into specific subcellular compartments remains problematic. Specific labeling of the cytoplasm with a fluorescent Ca^{2+} dye can be achieved by microinjection of individual cells with a membrane-impermeable form of the dye, reversibly permeabilizing the plasma membrane of a population of cells in the presence of the potassium salt form of the dye using scrape loading or osmotic techniques (*see* **ref.** *7* for a review). Microinjection is labor intensive, technically demanding, and does not allow the study of a large number of cells simultaneously. The latter approaches risk damaging cells and do not enable loading of subcellular compartments such as organelles with Ca^{2+} indicators.

Beginning in the 1990s, genetically targeted recombinant chemiluminescent and fluorescent biosynthetic Ca^{2+} sensors have been used with great success to study Ca^{2+} signaling ***(8–10)***. By utilizing specific targeting sequences that direct expression of the sensors to various locations within cells, Ca^{2+} biosensors have provided measurements of $[Ca^{2+}]$ in the cytoplasm, mitochondrial

Table 1
Properties of Synthetic Fluorescent Calcium Indicators

Target	Indicator	Type	K'_d (μ*M*)	X_1 (nm)	X_2 (nm)	M_1 (nm)	M_2 (nm)	Dynamic range
Cytosol	Fura-2	DWX	0.15–0.22	340	365; 380	510		13–25
	Indo-1	DWM	0.23	340		400	475	20–80
	Fluo-3	SW	0.4	488; 505		530		40–100
	Fluo-4	SW	0.34	488; 495		> 510		> 100
	Fura Red	DWX; DWM	0.14	420	480; 488	> 640		5–12
	Calcium Green	SW	0.19	488; 505		530		~ 14
	Calcium Orange	SW	0.185	550		575		~ 3
	Calcium Crimson	SW	0.185	590		615		~ 2.5
Endoplasmic reticulum	MagFura-2 (Furaptra)	DWX	25	340	365; 380	> 505		6–30
	MagFluo-4	DWX	22	488; 490		> 510		
Mitochondria	Rhod-2	SW	1	550		575		14–100
Plasma membrane	Fura-2FF	SW	38	340	365; 380	> 505		
	Calcium Green C18	SW	0.28	488; 510		530		~ 8

Abbreviations: DWX, dual-wavelength excitation ratiometric dye; DWM, dual-wavelength emission ratiometric dye; SW, single-wavelength dye.

Note: The dynamic range is the fold change in fluorescence intensity or the ratio of fluorescence values measured under conditions of saturating and low calcium concentrations. Note that Fura red is normally used as DWX (ratio 420/480) but can be DWM when coloaded into cells with Fluo-3 or Fluo-4 (ratio 530/640).

Source: Adapted from **refs.** *7*, *25*, and *26*.

matrix, endoplasmic reticulum lumen, Golgi complex, nucleus, secretory granule surface, caveolae, and cytoplasmic surface of the plasma membrane *(9,11–23)*. Genes encoding biosensors based on recombinant aequorin, a Ca^{2+}-sensitive bioluminescent protein, as well as mutants of green fluorescent protein can be readily transfected into cells. **Table 2** summarizes the biophysical properties of genetically targeted fluorescent Ca^{2+} biosensors.

Constructs encoding recombinant aequorin chimeras are available commercially and can be targeted to specific locations within cells. Aequorin measures $[Ca^{2+}]$ across a wide range (0.1–100 μ*M*). Unfortunately, the brightness of aequorin emission is very low compared with fluorescent indicators. Experiments are generally performed using cell suspensions or by integrating light signals from many cells grown as a monolayer. Imaging aequorin signals in single cells with current technology provides poor spatial and limited temporal resolution. Detection of aequorin luminescence requires photomultiplier tubes housed within light-tight containers or expensive high-sensitivity photon counting arrays. The light-generating reaction of Ca^{2+} with aequorin depends on coelenterazine, a cofactor that must be present during the experiments. In addition, aequorin molecules are irreversibly consumed by the reaction with Ca^{2+}. This raises two problems. First, prior to the Ca^{2+} measurements, cells must be incubated for prolonged periods of time in solutions that do not contain Ca^{2+}; this prevents consumption of aequorin by the high $[Ca^{2+}]$ in extracellular solutions. Second, irreversible consumption of the indicator induces a measurement artifact that mimics lowering of $[Ca^{2+}]$, thus limiting the amount of time for an experiment, especially when measuring Ca^{2+} signals from subcellular regions, which have high $[Ca^{2+}]$ such as the lumen of the endoplasmic reticulum.

Genetically targeted biosynthetic fluorescent Ca^{2+} sensors overcome many of the limitations encountered with synthetic and chemiluminescent Ca^{2+} indicators. First described in 1997 by Tsien and his colleagues, cameleons provide investigators the tools necessary to record Ca^{2+} signals from specific subcellular compartments *(9)*. Cameleons are fluorescent biosynthetic Ca^{2+} indicators constructed by inserting a Ca^{2+} sensor (*Xenopus laevis* calmodulin and M13, a calmodulin-binding protein) between two mutated forms of green fluorescent protein (GFP). Cameleon fluorescence is affected by differences in the concentration of Ca^{2+} that alter the amount of fluorescence resonance energy transfer (FRET) between mutant forms of GFP. This process is influenced by a Ca^{2+}-induced change in the conformation of calmodulin–M13, which, consequently, alters the relative angular displacement between the two mutant GFPs, bringing them closer together, for example, following an increase in $[Ca^{2+}]$. The increase in FRET is a direct function of $[Ca^{2+}]$. In contrast to cameleons, camgaroos and pericams do not utilize FRET; Ca^{2+} binding results in a direct electrostatic change in the environment of these circularly permuted fluorescent proteins, causing a Ca^{2+}-dependent shift in

Table 2
Biosynthetic Fluorescent Calcium Sensors

Target	Biosensor	Type	K'_d (μ*M*)	*n*	K'_d (μ*M*)	*n*	Dynamic range	Ref.
Cytoplasm	Cameleon-1	FRET	0.07	1.8	11	1	1.7–1.8	*9*
	Cameleon-1/E104Q	FRET			4.4–5.4	0.76	1.7–1.8	*9*
	Cameleon-1/E31Q	FRET	0.083	1.5	700	0.87	1.7–1.8	*9*
	Cameleon-2	FRET	0.07	1.8	11	1	1.7–1.8	*9*
	Yellow Cameleon-2 (YC2)	FRET	0.07	1.8	11	1	1.5	*9*
	Yellow Cameleon-2 (YC2)	FRET			1.24	0.79		*34*
	Yellow Cameleon-2.1 (YC2.1)	FRET	0.1	1.8	4.3	0.6	2	*15*
	Yellow Cameleon-2.1 (YC2.1)	FRET	0.2	0.62				*16*
	Yellow Cameleon-2.3 (YC2.3)	FRET					2	*13*
	Yellow Cameleon-2.12 (YC2.12)	FRET						*19*
	Yellow Cameleon-3.1 (YC3.1)	FRET			1.5	1.1	2	*15*
	Yellow Cameleon-3.2 (YC3.2)	FRET			1.5	1.1	1.85	*24*
	Yellow Cameleon-3.3 (YC3.3)	FRET			1.5	1.1	2	*13*
	Yellow Cameleon-6.1 (YC6.1)	FRET	0.11				2	*22*
	Yellow Red Cameleon-2 (YRC2)	FRET	0.2–0.4				0.1–0.4	*17*
	Cyan Red Cameleon-2 (CRC2)	FRET	0.2–0.4				0.1–0.4	*17*
	Sapphire Red Cameleon-2 (SapRC2)	FRET	0.2–0.4				0.1–0.4	*17*
	Camgaroo-1	CPSW			7	1.6	8	*24*
	Camgaroo-2	CPSW			5.5	1.24	7	*13*
	Ratiometric-Pericam (RPC)	CPDWX			1.7	1.1	10	*18*
	Flash-Pericam	CPSW	0.7	0.7			8	*18*
	Inverse-Pericam	CPSW	0.2	1			7	*18*

(Continued)

Table 2 ***(Continued)***

Target	Biosensor	Type	K'_d (μ*M*)	*n*	K'_d (μ*M*)	*n*	Dynamic range	Ref.
	G-CaMP	CPSW	0.235	3.3			4.5	*20*
	pGA	CRET			10			*8*
Endoplasmic Reticulum	Yellow Cameleon-3er (YC3er)	FRET			4.4–5.4	0.76	1.6	*9*
	Yellow Cameleon-4er (YC4er)	FRET	0.083	1.5	700	0.87	1.4	*9*
	Yellow Cameleon-4er (YC4er)	FRET	0.039	0.57	292	0.6		*34*
	Yellow Cameleon-4er (YC4er)	FRET			292	0.6	1.7	*12*
	Yellow Cameleon-6.2er (YC6.2er)	FRET						*22*
Mitochondria	Yellow Cameleon-2mt (YC2mt)	FRET			1.26	0.79	1.3	*34*
	Yellow Cameleon-2.1mt (YC2.1mt)	FRET						*34*
	Yellow Cameleon-3mt (YC3mt)	FRET						*34*
	Yellow Cameleon-3.1mt (YC3.1mt)	FRET			3.98	0.67	1.3	*34*
	Yellow Cameleon-4mt (YC4mt)	FRET						*34*
	Yellow Cameleon-4.1mt (YC4.1mt)	FRET	0.105	0.81	104	0.62	1.3	*34*
	Camgaroo-2mt	CPSW						*13*
	Ratiometric-Pericam-mt (RPC-mt)	CPDWX			1.7	1.1	10	*18*
Golgi	Galactosyltransferase-Yellow Cameleon-3.3 (GT-YC3.3)	FRET			1.5	1.1	2	*13*
Nucleus	Cameleon-2nu	FRET	0.07	1.8	11	1	1.7–1.8	*9*
	Yellow Cameleon-3.1nu (YC3.1nu)	FRET			1.5	1.1	2	*16*
	Yellow Cameleon-6.1nu (YC6.1nu)	FRET						*22*

	Ratiometric-Pericam-nu (RPC-nu)	CPDWX			1.7	1.1	10	***18***
Secretory Granules	Phogrin-Yellow Cameleon-2 (phogrin-YC2)	FRET						***11***
Caveolae	Caveolin-1-Yellow Cameleon-2.1 (CYC2.1)	FRET	0.26	1				***14***
Plasma Membrane	Neuromodulin-Yellow Cameleon-2.1 (NYC2.1)	FRET	0.26	1				***14***
	Ratiometric-Pericam-synaptosome associated protein of 25 kDa (RPC-SNAP25)	CPDWX			1.7	1.1		***21***

Abbreviations: CPSW, circularly permuted, single-wavelength excitation; CPDWX, circularly permuted, dual-wavelength excitation; CRET, chemilumenescence resonance energy transfer.

Note: Subcellular location, apparent dissociation constant (K'_d) for Ca^{2+} and Hill coefficient (n) is listed for the sensors. Cameleon-1, Cameleon-1/E31Q, Cameleon-2, Cameleon-2nu, YC2.1, YC4er, and YC4.1mt display biphasic Ca^{2+}-binding curves and high- and low-affinity Ca^{2+} binding. The reader should note that in some cases, investigators have determined K'_d and n values in vitro and in vivo and should consult the references for additional details. An estimation of the dynamic range of the sensors is provided. The dynamic range in this case is defined as the fold change in fluorescent ratio or intensity of the sensor exposed to nominally 0 *M* [Ca^{2+}] and saturating [Ca^{2+}] (10–20 m*M*). Biosensors constructed from circularly permuted mutations of EYFP, Camgaroo-1, Camgaroo-2, Pericams, and G-CaMP have a much higher dynamic range than the fluorescence resonance energy transfer (FRET) sensors.

fluorescence emission *(13,18,20,22–24)*. Ca^{2+} biosensors exhibit different biophysical properties, such as pH sensitivity and Ca^{2+} affinities, that enable measurement of Ca^{2+} signals in different cellular compartments using single- and dual-wavelength emission and excitation microfluorometry.

The choice of the most appropriate indicator or indicators and measurement systems for the experiments is dictated by several considerations, including the source or location of the Ca^{2+} signal to be studied and whether direct visualization of spatial changes in subcellular [Ca^{2+}] is necessary *(7,25–27)*. In addition, certain constraints specific to the cell type or tissue under study might be important. For example, relatively homogeneous loading of populations of dispersed adherent cells with synthetic Ca^{2+} indicators is readily accomplished using membrane-permeable fluorescent derivatives, but loading thick biological tissues such as explants of islets of Langerhans, which consist of clusters of 1000–3000 cells, is problematic. Dye compartmentalization can be a significant problem (ability to cross one membrane implies multiple membranes might be crossed if esterase activity is low; targeted probes could offer an advantage here). Moreover, in some cases, loading primary cultures of dispersed cells has proven difficult. In this chapter, we describe protocols we employ to measure [Ca^{2+}] spatio-temporal gradients in endocrine cell lines and islets of Langerhans.

2. Materials

What follows is a list of the basic items needed to perform quantitative imaging of Ca^{2+} signals in cells. We find that two laboratory areas are required for these experiments: an area to perform cell culture and preparation of solutions used in the experiments, and a separate area in the laboratory or small room devoted to housing the microscope and imaging system. For our experiments, the imaging studies are performed in a darkened room (~10 m^2) adjacent to the main laboratory. If space is limited, a small region of the laboratory can be darkened using black curtains suspended from the ceiling or a light-tight box can be constructed or purchased to fit over the microscope.

1. Laminar flow, tissue culture hood with ultraviolet (UV) light.
2. Temperature-regulated, humidified incubator.
3. 95% O_2: 5% CO_2 gas tanks (for bubbling bicarbonate-buffered perifusion solutions).
4. Complete cell culture medium.
5. Trypsin-EDTA cell dissociation solution.
6. Phosphate-buffered saline (PBS) without Mg^{2+} and Ca^{2+}.
7. Hemocytometer.
8. Tissue culture flasks or circular cell culture plates.
9. Six-well tissue culture plates.
10. Glass cover slips and coating reagent if required.

11. Pipet tips and micropipets.
12. Siliconized, 1.5-mL Eppendorf microcentrifuge tubes.
13. Serological pipets and handheld dispenser (1, 5, 10, 25 mL).
14. Fine-point jeweler's forceps.
15. Microperifusion system and chamber.
16. Temperature-regulated water bath and thermometer.
17. Peristaltic pump and tubing for perifusion system (various sizes; chemically resistant).
18. Vibration-free isolation table for microscope.
19. Pipette Aid motor or aquarium bubbler.
20. Two 500-mL vacuum Ehrlenmeyer flasks and rubber stoppers and desiccant.
21. Inverted or upright microscope equipped for epifluorescence (for standard wide-field fluorescence imaging), confocal laser scanning microscope, or spinning disk optical microscope.
22. Fluorescence objectives (×10, ×20, ×40, ×60, ×100).
23. Fluorescence light source (xenon or mercury) or laser.
24. Optical filters (neutral density, excitation, dichroic, and emission).
25. High-speed excitation and emission filter changing devices with computer-interfaced controller.
26. High-sensitivity, high-resolution cooled digital camera (charge-coupled device [CCD]).
27. Computer workstation with a 17- to 20-in. monitor, local area network access, high-capacity data storage peripheral devices (0.06–1 Tbyte capacity) for image and data archiving, and color printer.
28. Image acquisition and analysis software with appropriate video card and driver for CCD.
29. Chemical salts and buffers to prepare perifusion solutions, glass bottles, and conical centrifuge tubes.
30. Fluorescent Ca^{2+}-sensitive dyes (membrane permeable as well as potassium salt forms for performing in vitro calibration).
31. Mammalian expression plasmids encoding biosynthetic Ca^{2+} sensors.
32. Competent *Escherichia coli* strains for plasmid transformation, growth medium, sterile flasks, Luria–Bertani (LB) agar plates, transfer loop, bunsen burner, rotating temperature-regulated culture chamber.
33. Plasmid cDNA preparation kits.
34. Mammalian cell transfection reagents.
35. Ca^{2+} calibration reagents and buffers.

3. Methods

3.1. Tissue Culture

Our experiments are performed on endocrine cell lines and primary cells. For imaging studies using fluorescent synthetic or biosynthetic Ca^{2+} indicators, we seed cells onto uncoated glass cover slips in six-well tissue culture plates

24–72 h before the experiments; cells are maintained under normal culture conditions (*see* **Note 1**). Typically, we seed at a cell density to achieve 60–80% confluence by the day of the experiment in order to image [Ca^{2+}] transients in single cells and also to have sufficient cell-free regions to obtain background fluorescence measurements.

3.2. Synthetic Ca^{2+} Indicators

Lipophilic (membrane permeable) and hydrophilic (membrane impermeable) derivatives of synthetic fluorescent Ca^{2+} dyes can be obtained from many commercial sources. Membrane-impermeable Ca^{2+} indicators can be loaded into cells by microinjection, osmotic methods, or scrape-loading and remain in compartments into which they are introduced. They can also be used for in vitro calibrations. For our cell imaging experiments, we load cells with AM derivatives of the indicators (*see* **Note 2**).

3.3. Loading Cells With Synthetic Ca^{2+} Dyes

The basic protocol to load neuroendocrine cells with Fura-2, Fluo-3, Fluo-4, Calcium Crimson, Fura Red, Calcium Orange, Calcium Green, MagFura-2, and Rhod-2 is outlined here.

1. Using fine-point jeweler's forceps, we gently remove a cover slip from the six-well tissue culture plate and transfer it into a microperifusion chamber (Harvard Apparatus).
2. Cells are incubated in the chamber with Krebs-Ringer bicarbonate (KRB) or Krebs-Ringer HEPES (KRH) buffer solution containing 5 μ*M* AM form of the dye and 0.0125–0.025% Pluronic F127 (*see* **Note 3**). Cell loading is conducted for 15–20 min in a humidified CO_2/O_2 incubator at 37°C. Following this period of time, the microperifusion chamber is mounted onto the temperature-controlled specimen stage of an inverted fluorescence microscope equipped for either standard wide-field epifluorescence imaging or optical spinning disk laser confocal microscopy. The cells are rinsed for 15–30 min with KRB or KRH to remove all extracellular AM form of the dye and to provide time for complete de-esterification.

Evaluation of the quality of dye loading is essential. Whereas the use of AM membrane-permeable forms of fluorescent Ca^{2+} indicators enables large numbers of cells to be loaded simultaneously, assessment of the compartmentalization of the dye is essential for achieving reproducible results and for reliable interpretation of the imaging data. Dye loading is affected by AM dye concentration, loading temperature and time, and cell type. Several reviews are available that discuss in detail the evaluation of dye loading and optimization of loading conditions *(6,7)*. Optimal conditions for dye loading vary depending on cell type and must be determined empirically.

3.4. Expressing Biosynthetic Ca^{2+} Biosensors in Cells

Fluorescent Ca^{2+} biosensors are not yet available commercially. It has been our experience that, without exception, investigators who initially designed, constructed, and characterized a biosensor will provide samples of the plasmid constructs. In some cases, completing an interinstitutional materials transfer agreement will be required before obtaining the biosensors. The reader is urged to directly contact the investigator for procedures to obtain the constructs.

Following receipt of samples (usually 1–5 µL of a 1- to 2-µg/µL stock cDNA solution, we use commercial kits to produce larger volumes of the plasmid cDNA (Qiagen Maxi Prep) and to transiently transfect cells using liposomal methods. Cells are seeded onto 15-mm or 25-mm glass cover slips 1 d prior to transfection and incubated in complete growth medium. On d 2, cells are transfected with 1–2 µg of cDNA for 4 h (*see* **Note 4**). Imaging studies are performed 2–4 d after transfection.

3.5. Microperifusion

Precise control of the contents, temperature, and volume of the external bathing solutions is absolutely necessary to ensure reproducible experiments. Most investigators employ temperature-regulated, microperifusion chambers mounted on the specimen stage of inverted and upright fluorescent microscopes. Our experience indicates that continuous superfusion of cells with different solutions, rather than by direct, manual application of chemical reagents into the chamber and onto cells using micropipets, enables more precise control and reproducibility in altering experimental conditions.

In our studies, cells are constantly superfused by defined buffer solutions administered 2–5 mL/min; in a 1-mL microperifusion chamber, higher flow rates (>5 mL/min) could dislodge cells, whereas slower fluid flow (<2 mL/min) does not enable sufficiently rapid solution changes. Fluid flow is driven by peristaltic pumps or gravity flow. Temperature of the superfusate is maintained at 37°C. A steady rate of fluid removal from the chamber is maintained by a small plastic tube immersed in the chamber and attached to two 500-mL Erlenmeyer vacuum flasks connected in series. In one flask, the effluent is collected, whereas the other flask, proximal to the vacuum source, contains a desiccant that prevents contamination of the vacuum pump; negative pressure is provided by a fish tank or Eppendorf pipettor electric pump running in reverse mode. Alternatively, one could use a peristaltic pump with both perifusion chamber inflow and outflow matched for constant fluid levels. Experimental conditions are altered by changing the perifusate (*see* **Note 5**).

3.6. Measuring $[Ca^{2+}]_i$ Using Wide-Field Fluorescence Imaging

We utilize an inverted microscope equipped for multiparameter digitized video fluorescence imaging. Two perifusion systems mounted onto the specimen

stage of Nikon TE-2000U microscopes are used in our laboratory: Harvard/Medical Systems PDMI-2 Micro-Incubator and Warner Instruments Series 20 Open Bath Recording/Imaging Chambers. The chambers are connected to a TC-202A Bipolar Temperature Controller and dual-channel TC-344B Chamber System Heater Controller, respectively. The PDMI-2 system is used for experiments involving perifusion of bicarbonate-buffered solutions via a peristaltic pump, whereas the Warner chambers are used in studies in which the solutions are perifused by gravity flow and rapid laminar flow fluid exchange is required. Glass cover slips (25-mm circular) with cells loaded with synthetic Ca^{2+} indicators or expressing biosynthetic Ca^{2+} sensors are placed into a Teflon glass cover-slip holder. Two chambers are available for use with the PDMI-2 system. The MSC-TD (Harvard Apparatus AH 65-0051) has an optical window of 19 mm × 31.5 mm and 1 mL volume. The MSC-PTD has a small rectangular optical window 9.5 mm wide and 19 mm long, and volume less than 1 mL for fast fluid transfer. The modular design of the Warner Series 20 chamber system is very flexible, enabling a wide choice of chamber sizes and configurations. We use closed and open bath Series 20 imaging chambers. For small-volume chambers (36–70 μL), cells are cultured on 15-mm circular cover slips. Larger chambers (>100 μL) use 25-mm circular cover slips. Superfusion of cells is initiated immediately after placing them into the imaging chamber and maintained throughout the experiment.

The cells are visualized with a ×40 or ×60 oil-immersion fluorescence objective. Larger tissues such as single intact islets of Langerhans are studied using a ×10 or ×20 fluorescence objective. Objectives with a high numerical aperture and long working distance are preferred with inverted microscopes. If you use an upright microscope, a ×60 water-immersion objective is highly recommended for experiments with living cells.

A 75-W xenon or mercury bulb is used for conventional wide-field fluorescence imaging. Excitation light is attenuated with neutral-density filters and the excitation wavelength is controlled by optical filters. Currently, we employ a Sutter or Prior filter wheel to set excitation wavelengths. The filter wheel is attached to a filter/shutter control device connected to a computer. Image acquisition and analytical software controls filter wheel settings and shutter activity. A separate emission filter wheel is utilized to change emission light wavelengths and to perform multiparameter emission microphotometry.

Fluorescent signals from cells are captured with an intensified video camera or a digital CCD. There are many cameras available for fluorescence microscopy. Because of space limitations, we will not review the wide range of digital cameras here. The choice of camera depends on resolution and acquisition speed requirements as well as spectral properties. The reader is encouraged to investigate individual specifications of the digital cameras currently

available from manufacturers' websites for additional information. A video camera is suitable for Fura and some single-wavelength dyes, but the limited 8-bit digitization range makes it ill-suited for FRET probes as well as dyes with high dynamic response, such as Fluo-3 and Fluo-4.

3.6.1. Measuring $[Ca^{2+}]_i$ Using Fura-2

1. Make all experimental solutions fresh daily for imaging studies. Pre-equilibrate solutions to required temperature, and if bicarbonate-buffered perfusates are used, then bubble solutions with $O_2 : CO_2$ gas 15–30 min before experiments.
2. Remove cover slips with monolayers of cells from multiwell tissue culture plates and place them into the microperifusion chamber.
3. Load cells with Fura-2AM. We limit exposure of Fura-2 to bright light in the laboratory, and we load cells with Fura-2 either in a cell incubator with bicarbonate buffered solutions or, if loading at room temperature with HEPES-buffered solutions, use a light-tight box. See above comments about loading conditions. Do not use bicarbonate buffers in room air.
4. During Fura-2 loading, set the controller for the desired chamber temperature. Make certain that all fluids flow freely in all tubing. Degassing of solutions in tubing can form bubbles that restrict/occlude flow. Adjust and set fluid inflow rate. Set acquisition parameters using image acquisition and analysis software. Set excitation filter wavelengths (using the image acquisition software). For Fura-2, use 340-nm and 380-nm excitation filters, 400DCLP dichroic mirror, and 510/40-nm emission filter. For typical experiments, we record image pairs (exposure time of 50–250 ms for each excitation wavelength) at 0.20- to 10-s intervals. Set the shutter to automatically close between image pair exposures to reduce the amount of time cells are exposed to UV light. The duration of our experiments varies from 5 min to 2 h. It is important to completely plan the acquisition profile prior to running an experiment, and some software packages allow users to program and store protocols for experiments. This can greatly simplify the procedures during an experiment and aid in repeating experimental protocols with precision.
5. Mount chamber onto the microscope stage and immediately begin rinsing cells for 10–15 min with standard external solution to remove excess Fura-2AM. Adjust and set fluid efflux rate to match influx rate. This prevents large fluctuations in perifusate volume in the chamber. Make certain to maintain a constant vigil on the status of the fluid efflux from the chamber in order to prevent overflow accidents, which can severely damage an inverted microscope and the objectives.
6. Prior to exposing cells to excitation light, preliminary focus can be accomplished using bright-field light and the binocular eyepieces. Be certain to focus the objective with great caution. Approach the cover slip with the objective slowly; once the oil has contacted the surface of the cover glass, make adjustments only with the fine-focus controller. Do not extend the objective too far. Impacting the cover glass with the metal surface of the objective will break the cover glass; the cover slips are extremely fragile and remarkably little force is required to shatter them with the objective. Not only will this cause loss of a potentially important biological

sample, but it also risks severe (and quite costly!) damage to the internal components of the microscope because of contamination with saline solutions. For most cells, we set the focal plane about halfway through the cells.

7. Insert a neutral-density filter (Chroma UV filters, 0.3–2.0) into the excitation light path before opening the excitation light shutter (*see* **Note 6**).
8. Open the shutter and visualize cells using fluorescent excitation light. Choose an appropriate field-of-view. Use the acquisition software to refocus using either the 340-nm or 380-nm excitation light. In general, we use the 380-nm illuminated cells for focus because this generally is a brighter image than the 340 nm. Next, set the camera gain. This can be accomplished using either a peripheral camera illumination controller or the camera gain controls in the image acquisition software (*see* **Note 7**). Once set, the camera gain is not readjusted during the experiment. It is important to be consistent here because arbitrary gain changes can affect conversion of ratio values to ion concentration unless in vivo calibrations are used. Finally, use the acquisition software to delineate regions of interest (ROIs) in which imaging data are collected and displayed during the experiment. These can consist of individual cells, groups of cells, and/or subcellular regions in one or multiple cells.
9. Recheck the experimental protocol, acquisition settings, perifusion solutions, fluid flow, and image focus. Begin the experiment, changing experimental conditions as required. During each experiment, we simultaneously display the 340-nm, 380-nm, and ratio images and graphical depictions of the time-dependent changes in ratio values.
10. A cell-free or in vitro calibration method can be performed to convert the F_{340}/F_{380} ratio into molar $[Ca^{2+}]$. A calibration curve plotting the F_{340}/F_{380} ratio as a function of $[Ca^{2+}]$ can be used to provide an estimate of $[Ca^{2+}]_i$. To construct the curve, the F_{340}/F_{380} ratio is measured in a series of buffered solutions with defined $[Ca^{2+}]$ and the potassium salt of Fura-2 (usually 1–5 μ*M*). This calibration method, however, does not take into account possible effects of intracellular environment on Fura-2 ***(6)***. At the end of each experiment, we perform an in vivo (or *in situ*) calibration. To determine the fluorescence intensity values at saturating $[Ca^{2+}]$, the cells are exposed to 10–20 μ*M* ionomycin in the presence of extracellular Ca^{2+}. Under these conditions, the fluorescence maximum value for the intensity ratio is reached in about 30–60 s. After this, ionomycin, in solutions containing 10–20 m*M* EGTA and no added Ca^{2+}, is applied. The amount of time required to reach the minimum fluorescence intensity for the ratios varies and can take 5–60 min before reaching a steady-state value. Some labs prefer to use 4-Br-A23187 as the ionophore because it aids in setting R_{min}. Do not use the nonbromonated form of this ionophore because its intrinsic fluorescence will interfere with the calibration of Fura-2. To convert the fluorescence intensity ratio into molar $[Ca^{2+}]$, we use the following equation ***(1)***:

$$[Ca^{2+}] = K'_d \beta [(R - R_{min})/(R_{max} - R)]$$

where K'_d is the relative Ca^{2+} dissociation constant of Fura-2 (150–220 n*M*), β is the ratio of the 380-nm fluorescence intensity recorded at 0 and saturating $[Ca^{2+}]$, R is the ratio of Fura-2 fluorescence intensities at 340 nm and 380 nm, R_{max} is the fluorescence ratio at saturating $[Ca^{2+}]$, and R_{min} is the fluorescence ratio at 0 $[Ca^{2+}]$.

11. We save all images to the computer hard drive and program the software to automatically export and save the intensity data to spread sheets. After each experiment, the data and images are archived onto CD-R or DVD-R storage media for offline analysis at computer workstations in the main laboratory. Also, the computers in the imaging suite are networked to the workstations to facilitate downloading experimental data to offline sites. At the end of each session, we suggest deleting imaging files or transferring them to CD-R or DVD-R storage media because they can rapidly fill most computer hard drives with 60–80 gigabytes storage capacity.

3.7. Measuring $[Ca^{2+}]_i$ Using Laser Scanning Confocal Microscopy

Confocal laser scanning microscopy (CLSM) allows visualization of subcellular $[Ca^{2+}]$ gradients with high spatial and temporal resolution. The primary advantage of CLSM over standard, wide-field epifluorescence imaging is the reduction of fluorescence emission that originates from outside the plane of focus. The contribution of out-of-focus fluorescence reduces image contrast and resolution of fine microanatomical structures, confounds interpretation of quantitative imaging experiments, and hinders visualization of signaling events occurring within specific subcellular locations. This can be especially problematic in thick biological samples, such as intact single pancreatic islets of Langerhans (which are spherical clusters of cells 100–300 μ*M* in diameter consisting of 1000–3000 cells) or in tissue slices. An example of this artifact is illustrated in **Fig. 1** (see Color Plate 1, following p. 274), which shows the distribution of Fura-2 fluorescence in mouse islets of Langerhans in vitro; Fura-2 fluorescence appears to be present throughout the islet cells. CLSM images from a consecutive series of optical *z*-axis sections through a Fura-2-loaded mouse islet however clearly reveal that Fura-2 fluorescence is confined to the outer cell layers of the islet and not present within the core of the islet (*see* **Fig. 2**).

Single-wavelength excitation and ratiometric dual-wavelength emission imaging can be conducted with CLSM. Although a wide range of fluorescent Ca^{2+} indicators and genetically targeted Ca^{2+} biosensors are available for CLSM, most studies have utilized single-wavelength excitation Ca^{2+}-sensitive dyes such as Fluo-3 or Fluo-4. The choice of a specific Ca^{2+} indicator depends on the laser excitation wavelengths available. Many CLSM systems utilize an argon–krypton laser light source, which produces three discrete excitation lines: 488 nm, 568 nm, and 647 nm. Alternatively, many confocal systems use argon and He–Ne lasers (488- and 543- or 633-nm lines). Until recently, UV laser sources were uncommon because the lasers required high power and suffered from short life. Solid-state diode lasers are now available that could soon expand the wavelengths available in laser-based confocal systems.

It is reasonable to question the need for ratiometric imaging for quantitative measurements of $[Ca^{2+}]$ in confocal systems because the in-focus volume, which can be many voxels (three-dimensional pixels), is a constant and much

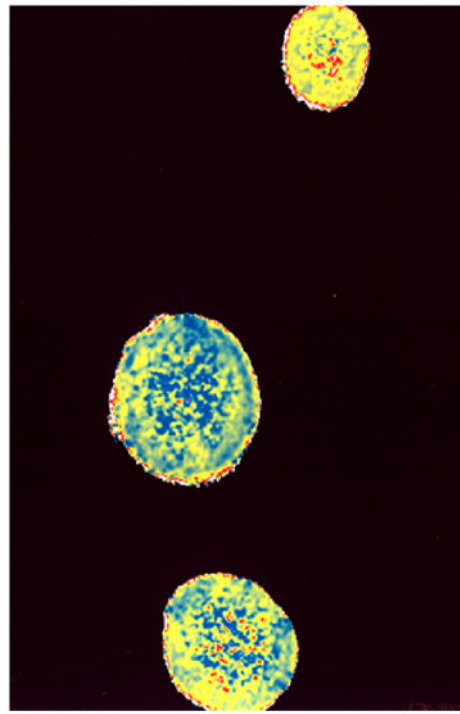

Fig. 1. Pseudocolored image of mouse islets loaded with Fura-2. The islets were imaged by conventional wide-field epifluorescence using a ×10 objective. The apparent distribution of the Fura-2 fluorescence throughout the islets is an artifact resulting from the contribution of fluorescence from above and below the focal plane. (*See* Color Plate 1, following p . 274.)

less than the volume of a cell. The main rationale is to account for dye dilution caused by changes in cell volume during measurements ***(25,28–30)***. Most scanning confocal systems contain at least two emission detector channels that permit emission ratio-based measurements. Emission ratio dyes like Indo-1 can be used in confocal imaging. Also, one can perform ratiometric imaging of cells coloaded with dyes that increase and decrease fluorescence intensity with $[Ca^{2+}]$, such as Fluo-3 and Fura red, respectively. With appropriate sets of dichroic and emission filters, simultaneous recordings of fluorescence emission intensities (stimulated by a single wavelength of excitation light) from cells loaded with multiple Ca^{2+}-sensitive dyes (e.g., Fluo-3 and Fura red) have been used to perform ratiometric dual-wavelength emission measurements of $[Ca^{2+}]$ ***(28–30)***. Excitation-ratio dyes like Fura-2 are not used because appropriate UV lasers are not commonplace and fast excitation line selection and switching requires expensive hardware.

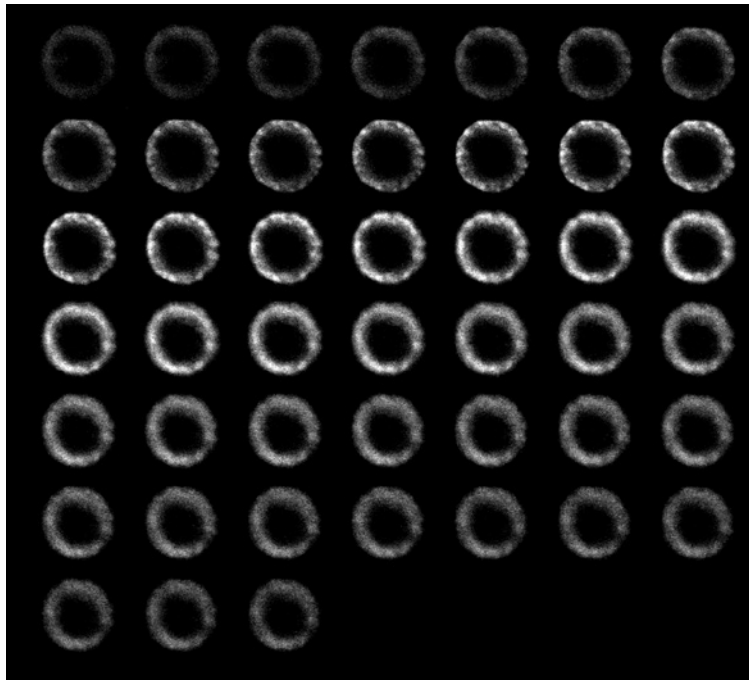

Fig. 2. Serial optical *z*-sections of a mouse islet loaded with Fura-2. The islet was imaged using a UV confocal scanning laser microscope. Note the annular fluorescence and the absence of fluorescence within the central regions of the islet. Spacing between each section was 1 μm.

Ca^{2+} signals can be studied using the confocal microscope operating in one of three possible imaging modes. The single line-scanning mode (*xt*-scanning, where *x* represents a line one pixel wide and *t* is time in seconds) provides the highest temporal resolution. Depending on scanner design, line sample rates range from about 667 to 4000 lines/s. In this mode, the laser beam rapidly and repeatedly scans along the line across the same region of an optical field. This approach has greatly facilitated the study of elementary Ca^{2+} signals and the initiation and propagation of intracellular Ca^{2+} waves ***(27)***. More recently, new CLSM systems allow for multiple lines (and different shapes) to be employed in *xt*-scanning. It is important to minimize laser intensity because bleaching and photodamage are especially high as a result of the energy being confined to tiny cell volumes. A common solution might be to decrease confocality by opening the system pinhole(s).

Analogous to the wide-field epifluorescence method described earlier, spatio-temporal [Ca^{2+}] gradients in a thin optical section of cells can be imaged using the *xyt*-scanning mode. Although the temporal resolution using *xyt*-scanning is

slower than line-scanning, more spatial information can be collected. Confocal imaging systems allow the operator to adjust the scanning rate, sampling density, and size of the optical area for *xyt* imaging of biological samples. Temporal and spatial resolution is dependent on the laser scanning speed: the slower the scan rate, the lower the temporal resolution, the brighter the image (up to the point where all dye molecules have been excited), and the higher the spatial resolution (increased pixel dwell time decreases the impact of detector noise). Excessively slow scans will rapidly bleach the probes and will cause photodamage. Because the images in the *xyt*-scanning mode are confocal, contribution of fluorescence from outside the focal plane is minimized; this important optical property greatly facilitates the identification of Ca^{2+} signals originating from different subcellular compartments with precision. Requirements for spatial and temporal resolution will dictate the type of confocal to be used for *xyt*-scanning. If high temporal resolution is required (such as that necessary to visualize initialization and propagation of Ca^{2+} waves through the entire cell or a collection of cells), then high frame or image acquisition rates should be employed. Standard galvanometer mirror-scanning confocal microscopy systems can scan a full frame (512×512 pixels) in approx 1 s and are capable of 10- to 30-Hz scanning small *xy* regions (e.g., 64×64 and 128×128 pixels). However, the image intensity and contrast are low and spatial resolution is limited. A better solution for high-speed, high-resolution imaging is to use a spinning disk confocal microscope and image capture using high-sensitivity, high-speed CCD digital cameras. These microscopes are capable of data acquisition rates between 30 and120 Hz with excellent full-frame spatial resolution. One disadvantage is that these systems typically are designed to acquire a single emission wavelength. Acquisition of multiple emission images either requires multiple CCD detectors or a device to record all wavelengths on different portions of the same camera chip.

The third mode, *xyzt*-scanning, allows resolution of spatio-temporal $[Ca^{2+}]$ gradients in the volume of the cell. Dynamic three-dimensional cell imaging involves repeated and rapid acquisition of *xy* images in multiple *z*-axis optical sections over time. The changes in *z*-axis steps can be accomplished by (a) a stage-stepping motor attached to the focus knob that precisely and reproducibly alters the position of the microscope stage, (b) an intrinsic/internal motorized focus (on some automated microscopes), (c) a high-speed piezoelectric device that controls the position of the viewing objective without moving the microscope stage, or (d) a galvanometer stage plate that can accurately displace the stage up to approximately 100 μ*M*.

3.7.1. Measuring $[Ca^{2+}]_i$ by CLSM in the Line-Scanning Mode

1. Grow cells on cover slips and load with single-wavelength excitation Ca^{2+}-sensitive fluorescent dyes (e.g., Fluo-3 or Fluo-4). Place the coverslip into a microperifusion chamber mounted on the specimen stage of the confocal microscope

system and superfuse cells with buffers for 15–30 min to remove excess indicator. Initial focus of the cells should be accomplished using condenser light.

2. Use *xy* scans to identify the cell or cells to be studied. Refocus the image under fluorescent laser excitation light (for Fluo-3, excitation line 488 nm from the Ar/Kr laser and emission wavelength detected at 510–530 nm). Set the gain (30–60% pixel saturation), black levels, and pinhole/slit width. Use minimal laser power settings (1–10%) to avoid photobleaching and phototoxicity. Configure the line-scanning acquisition in accordance with the CLSM system you are using; adjust position of the line (or lines) as required.
3. Begin the experiment. For rapid solution exchanges, we suggest using a gravity-fed perifusion system or microspritzer devices.
4. Archive the data for offline analysis. A wide choice of imaging software is available for offline analysis of line scan data. Data can be expressed as a ratio of the pixel fluorescence intensity (F) along the line scan measured at each time-point relative to baseline (F_0). The pseudoratio value (F/F_0) represents the foldchange in F relative to F_0 and can be converted to $[Ca^{2+}]$ by the equation ***(1,31)***:

$$[Ca^{2+}] = K'_d\,[(\beta F/F_0) - (1/\alpha)]/(1 - \beta F/F_0)]$$

where K'_d is the apparent Ca^{2+} dissociation constant of the dye, α is the ratio of F_{max}/F_{min}, and β is the ratio of F_0/F_{max}. F_{max} is the maximum fluorescence intensity value (following application of 10 µM ionomycin) and F_{min} is the minimum fluorescence intensity in the absence of Ca^{2+} (10 µ*M* ionomycin, 10–20 m*M* EGTA, and no added Ca^{2+}). The data can be displayed as an image consisting of a combined collection of the consecutive line scans showing the changes in F, $[Ca^{2+}]$, or R (depicted in gray scales or pseudocolored, respectively) or graphically, expressing the pseudoratio, R, or $[Ca^{2+}]$ as a function of time.

3.7.2. Single-Wavelength Excitation Measurements of $[Ca^{2+}]_i$ Using CLSM

1. Grow cells on glass cover slips and load with single-wavelength Ca^{2+} indicator. Like the line-scanning experiments, the fluorophore of choice for *xyt*-scanning is Fluo-3 or Fluo-4, although many others are commercially available. Fluo-3 fluorescence intensity is very low at resting baseline $[Ca^{2+}]_i$ (50–100 n*M*) and increases 4-fold to 10-fold at saturating $[Ca^{2+}]$. We typically load cells in KRB or KRBH containing 1–5 µ*M* Fluo-3/AM for 15–20 min at room temperature or at 37°C.
2. After the dye loading, wash cells with extracellular solutions for 10–20 min by continuous superfusion.
3. Set up the confocal excitation and emission wavelengths, and adjust photomultiplier gain, slit width, and black levels in accordance with the confocal system operator's guide. Identify a field-of-view with sufficient number of cells and a cell-free area for background ROI. Use acquisition software to create ROIs that can consists of single cells, cell clusters, or single or multiple subcellular regions. Set up the acquisition program (duration of experiment, number of images to be acquired, and online graphical plotting formats, if available).

4. Perform the experiment and, afterward, conduct an in vivo calibration. Be sure to carefully monitor fluid exchange in the microperifusion chamber to avoid accidental flooding and exposure of microscope to saline solutions. If an accident does occur, immediately cease the experiment. Dry the microscope with absorbent paper, lightly cleaning all affected surfaces with a pad of absorbent paper moistened with distilled water. If saline solution has entered the body of the microscope or the interior of an objective, do not hesitate to contact the microscope technician for immediate cleaning and repair. Objectives used on confocal microscopes can easily cost over $10,000 each and can be seriously damaged if saline solution is wicked inside them. Let the system administrator determine whether fluid has entered any part of the system.
5. Imaging data are stored and analyzed as earlier.

3.7.3. Dual-Wavelength Ratiometric Emission Measurements of $[Ca^{2+}]_i$ Using CLSM

1. Culture cells on cover slips. Load cells with Fluo-3/AM and Fura red/AM for 15–20 min at room temperature or at 37 ºC. Fluo-3 and Fluo-4 produces a much brighter signal than Fura red. For loading rat hepatoma cells, we used a 1:3 ratio of Fluo-3/AM and Fura red/AM For other cell types (mouse insulinoma cells), we used a 1:5 ratio.
2. Rinse cells 15–30 min with perifusate by continuous superfusion. During this time, perform the initial focus, identify a field-of-view, and set up the confocal system and data acquisition; identify ROIs and remember that the ROI used for background subtraction should be located in a cell-free area. Both dyes are excited by the 488-nm line of an Ar or Ar/Kr laser, and emission intensities are monitored simultaneously at 535 nm (Fluo-3) and 622 nm (Fura Red) (*see* **Note 8**). Recheck focus before performing the experiment.
3. Conduct the experiment, monitoring the status of the perifusion system throughout.
4. Save image and data files to CD-R or DVD-R storage media. Background-subtracted data can be expressed as the time-dependent change in the ratio of Fluo-3 (FI_{FL3}) and Fura Red (FI_{FR}) fluorescence intensity: As $[Ca^{2+}]$ increases, FI_{FL3} and FI_{FR} increase and decrease, respectively. Converting FI_{FL3}/FI_{FR} into $[Ca^{2+}]$ can be accomplished using in vivo calibration *(28,29)*.

3.8. Measuring $[Ca^{2+}]$ in Organelles

Ca^{2+} signaling is regulated by localized control of Ca^{2+} fluxes. To fully define and understand subcellular Ca^{2+} signaling, the contribution of the $[Ca^{2+}]$ within organelles must be directly studied. $[Ca^{2+}]$ gradients in mitochondria and endoplasmic reticulum (ER) have been imaged using synthetic Ca^{2+} indicators Rhod-2 and MagFura-2, respectively, and are loaded into cells using AM derivatives of the dyes. Cationic Rhod-2 partitions into mitochondria because of inner mitochondrial membrane hyperpolarization. Mag-Fura-2 (or Furaptra) has a low affinity for Ca^{2+}, thus making it a suitable indicator of Ca^{2+} fluxes in

regions of high [Ca^{2+}]. This indicator, however, distributes throughout the cytosol and organelles, depending on loading conditions (low temperature favors dye compartmentalization because esterase activity is lowered while diffusion rates are not appreciable affected). Measurements of ER Ca^{2+} fluxes with Mag-Fura-2 are generally conducted in permeabilized cells in order to eliminate the contribution of fluorescence originating from the dye distributed in the cytosol. Alternatively, cells are incubated at 37°C for as long as overnight to allow transporters to clear the cytosol of indicator. Mag-Fura-2 has been used to detect ER Ca^{2+} signaling in intact cells. This involves loading cells with the AM form of the indicator, followed by an overnight incubation in growth medium (without Mag-Fura-2/AM), during which time cytosolic but not organelle-sequestered Mag-Fura-2 is removed by plasma membrane anion transporters.

Genetically targeted Ca^{2+} biosensors represent the most recent approach to directly image intraorganelle Ca^{2+} signals. Recombinant forms of aequorin and fluorescent fusion protein chimeras have been expressed in a wide range of eukaryotic cells. By including a targeting sequence in the expression vector, the Ca^{2+} biosensors can be expressed selectively in specific subcellular compartments such as the ER, mitochondria, Golgi, and nucleus. Single-wavelength excitation, dual-wavelength excitation, and dual-wavelength emission microspectrofluorometry can be used to quantitatively image subcellular Ca^{2+} signaling with genetically targeted fluorescent biosynthetic Ca^{2+} sensors. Although wide-field and confocal imaging can be used, we recommend CLSM or spinning disk optical confocal imaging because these approaches allow for the more reliable identification of the location of the fluorescent signal than standard wide-field imaging. This is especially important if the goal of a study is to record mitochondrial flux vs cytosolic (or ER) fluxes (*see* **Note 9**).

3.8.1. Quantitative Dual-Wavelength Ratiometric Imaging of $[Ca^{2+}]_{organelle}$ Using Cameleon and Ratiometric Pericam Ca^{2+} Biosensors

1. Culture cells onto glass coverslips the day before transfecting with the biosensors. In 6-well culture plates, we seed each well (containing a 25-mm circular glass coverslip) with 0.5-1 $\times$ 10^6 cells.
2. Day 2, transfect cells with 1–2 µg DNA per well. There are several choices for gene transfer and the most optimal reagent or method will depend on cell type. We have used liposomal methods for transiently transfecting insulin-secreting cell lines, hepatoma cells, neuroendocrine cell lines, and primary vascular smooth muscle cells; the transfection efficiency ranged between 5 and 30%.
3. We perform imaging experiments with the transfected cells 48–96 h after transfection using conventional wide-field or single-spinning disk confocal microfluorometry to measure spatio-temporal [Ca^{2+}] gradients in the cytoplasm, ER,

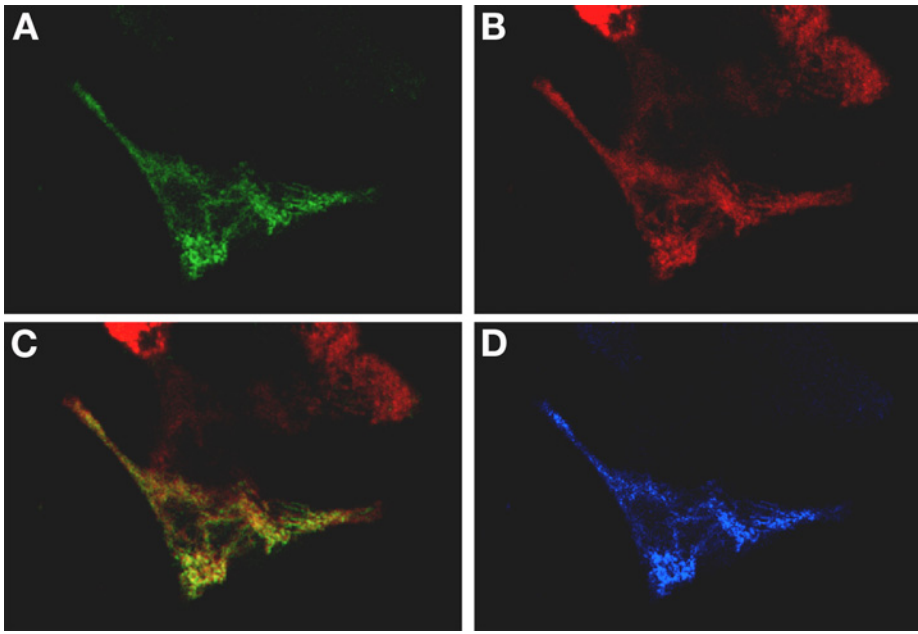

Fig. 3. Expression of mitochondrially targeted ratiometric pericam (RPC-mt) in neuroendocrine cells. Laser scanning confocal images of AtT20 cells colabeled with **(A)** RPC-mt (green) and **(B)** MitoTracker Red. **(C)** An overlay image constructed using Adobe Photoshop. The yellow color indicates colocalization of the two dyes. Note that some cells in the field-of-view do not express RPC-mt and remain red in the overlay image. **(D)** Map of colocalization using Bio-Rad confocal image processing software. Blue indicates regions of overlap between green and red channel fluorescence. (*see* Color Plate 2, following p. 274.)

mitochondria, or nucleus. The subcellular distribution of biosensors targeted to the mitochondria (*see* **Fig. 3;** Color Plate 2, following p. 274) and ER (*see* **Fig. 4**) can be easily visualized with confocal imaging. An example of real-time measurements of $[Ca^{2+}]$ oscillations in the cytoplasm of an insulin-secreting βTC3 cell expressing YC2.1 is shown in **Fig. 5**. Note the inverse relationship between the intensities of the FRET donor (*see* **Fig. 5**, top panel) and FRET acceptor (*see* **Fig. 5**, middle panel). For imaging cameleons, we recommend 436–440 nm excitation, 455DCLP dichroic, and 485 nm and 535 nm emission. Preferred filters for the ratiometric pericams are 410–415 nm and 480–485 nm excitation, 505DRLP-XR dichroic, and 535 nm emission. *See* **Table 3** for filter sets. To minimize photobleaching (and phototoxicty), we insert neutral-density filters into the excitation light path; attenuation of light between 50 and 99% seems to work best for the biosensors. We choose cells with intermediate brightness to study; in our experience, brightly fluorescent cells tend to be unresponsive, possibly reflecting an adverse effect of overexpression of the calmodulin-containing biosensor and buffering of Ca^{2+} transients ***(16)***. A

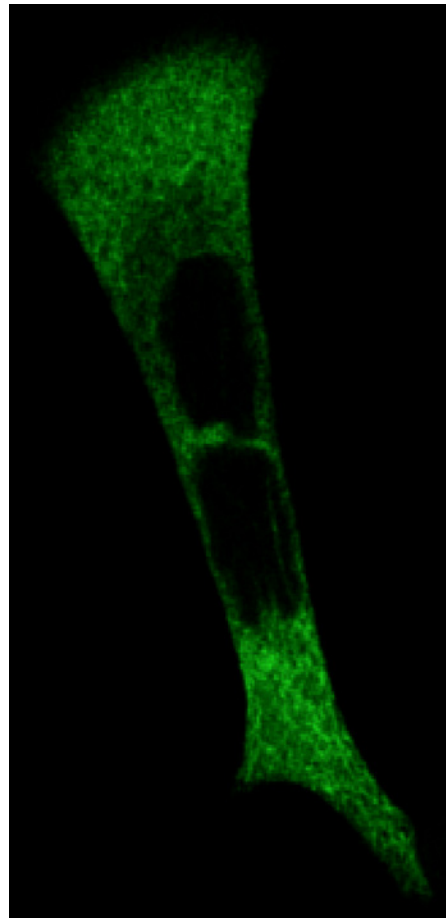

Fig. 4. Confocal micrograph of AtT20 cells expressing YC4er. Cells were transfected with YC4er using lipofectamine and imaged 2 d after transfection. Note the reticular pattern of distribution of the biosensor throughout the cells and absence of expression in the nuclei. Image obtained with a Bio-Rad 1024 MRC confocal laser scanning system mounted on an upright fluorescence microscope and a 60× water immersion objective using 488-nm excitation and 520-nm emission.

protocol to estimate the intracellular concentration of the biosensor has been described by Miyawaki and his colleagues ***(16)***.

4. We convert the ratio data into a molar value of $[Ca^{2+}]$ by in vivo calibration using 10 µ*M* ionomycin in the presence and absence of Ca^{2+} (plus EGTA). For the ER cameleon calibration, we add ionomycin in the presence of 10–20 m*M* $[Ca^{2+}]$ in the extracellular solution to evoke maximum ratio, then for minimum ratio, we administer an extracellular solution containing 10–20 m*M* EGTA and no added Ca^{2+}. The data are converted to molar $[Ca^{2+}]$ using the following equation ***(16)***:

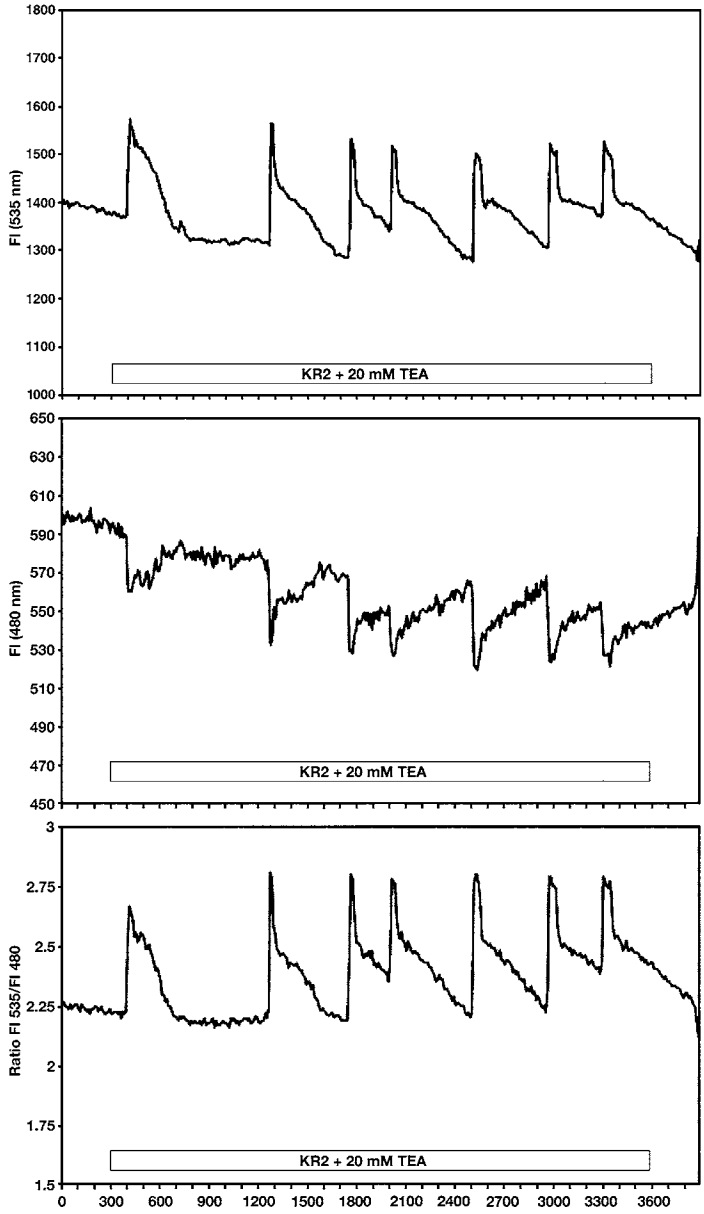

Fig. 5. [Ca^{2+}] oscillations in the cytoplasm of a βTC3 cell expressing YC2.1. The oscillatory changes in fluorescence intensity of the FRET acceptor (upper panel; FI535), FRET donor (middle panel; FI480), and ratio (lower panel; Ratio FI 535/480) induced by glucose (KR2; 2 m*M*) and tetraethylammonium (TEA) (open bar) were measured using conventional wide-field fluorescence microscopy. YC2.1 excitation was 440 nm; FRET donor and acceptor emissions were recorded at 480 nm and 535 nm, respectively. Time (s) is indicated on the *x*-axis.

Table 3
Filters for Imaging Fluorescence Calcium Biosensors

Biosensor	X_1	X_2	DC	M_1	M_2
Yellow Cameleon	440DF10		455DRLP	480DF30	535DF25
Red Cameleon					
YRC2	480DF10		505DRLP	535DF25	565EFLP
CRC2	440DF20		455DRLP	480DF30	565EFLP
SapRC2	400DF15		455DRLP	510WB40	565EFLP
Camgaroo	480DF30		505DCLP	535DF25	
Pericam	480DF10	410DF10	505DRLP-XR	535DF25	

Note: Our suggestions for excitation (X_1 and X_2), dichroic (DC), and emission (M_1 and M_2) filters for biosynthetic Ca^{2+} biosensors. Consult filter manufacturer for product details and recommended alternatives.

$$[Ca^{2+}] = K'_d\,[(R - R_{min})/(R_{max} - R)]^{(1/n)}$$

where K'_d is the apparent dissociation constant and n is the Hill coefficient. Published values for biosensor K'_d and n are summarized in **Table 2**.

4. Notes

1. Prior to seeding cells, cover slips are cleaned and sterilized in absolute ethanol, air-dried while exposed to UV light in a tissue culture hood for 1 h. Coating cover glasses with substrates, such as poly-L-lysine or collagen, is not required for attachment and growth of the cells we study. However, this is not the case for all cell types and use of coated glass cover slips might be necessary. The size and shape of the cover slips depends on the specimen chamber that will house the samples on the microscope stage of the imaging system. We use Harvard Apparatus and Warner Instruments microperifusion chambers. For the Harvard MP-4 system, the microperifusion chamber employs 25-mm circular glass cover slips, whereas 15-mm circular cover glass is used in the Warner PC-21 microperifusion system.
2. Manufacturers provide detailed instructions regarding storage, stability, reconstitution conditions, and handling precautions for the indicators. Unless instructed otherwise, we recommend that immediately upon receipt, the AM form of the dye be frozen at –20°C in a desiccator until ready for resuspension. Acetoxymethyl ester dye derivatives are shipped in multiple vials or a single vial containing 50 µg or 1 mg, respectively, and are soluble in dimethylsulfoxide (DMSO), ethanol, or methanol. Our common practice is to obtain multiple vials of the dye (50 µg per vial) and reconstitute the dye on the day of the experiments. We use water-free DMSO (stored at room temperature in a desiccator) to dissolve the membrane-permeable form of the dye to yield a final concentration of 1 m*M* (e.g., 50 µl DMSO/50 µg Fura-2AM; M_r = 1002). This volume and concentration provides enough indicator to load cells on 10–50 cover slips. The reconstituted AM form of the dye can be frozen and reused. Although repeated

freeze–thawing cycles do not seem to affect Fura-2, Fluo-3, and Fura red loading or fluorescent properties, we advise using newly reconstituted AM batches of the indicator at least once per week.

3. Pluronic is a nonionic detergent that helps to evenly disperse the AM form of the dye in an aqueous solution. Alternatively, bovine serum albumin can be used to keep the AM esters in solution; AM has limited aqueous solubility and precipitated dye will not enter cells, causing poor loading. Thus, increasing the dye concentration thus can decrease loading if the dye begins to precipitate. Precipitated dye is typically seen as bright debris over the surface of the cells and cover slip that rapidly bleaches from view. Metabolism of the cleaved AM moiety can produce toxicity in some cell types.
4. We have found that time in culture is a critical factor that determines transfection efficiency when using a lipofectamine method: a 12- to18-h culture period prior to transfection appeared optimal for cell types we have studied, including insulinoma, pituitary, and hepatoma cell lines. Even so, the maximum transfection efficiency we have achieved by the liposomal approach was approx 30% and ranged from 5 to 30%. Transfection of primary cells like pancreatic β-cells and rodent vascular smooth muscle cells with a liposome-based method was problematic, usually yielding an extremely low transfection efficiency. An alternative approach is to transfect cells with the biosensors using a viral-mediated gene shuttle vector. This requires construction of a viral vector because most of the biosensors are currently available as a plasmid cDNA. Notwithstanding this limitation, transfection efficiency is greatly improved (80–90%) and allows expression of the sensors in cell lines and primary cells as well as more complex biological tissues such as brain slices, pancreatic islets of Langerhans, and vascular preparations. Another key advantage of viral transfection is the potential for selective expression of a biosensor in a specific cell type within a multicellular tissue. This is accomplished by infecting tissues with viral vectors whose expression is under the control of a cell-specific promoter. For example, by driving adenovirus- and baculovirus-mediated expression with the rat insulin promoter sequence (RIP1), we have selectively and specifically labeled pancreatic β-cells in intact mouse islets of Langerhans with GFP-labeled fusion proteins. Finally, although it is conceivable that a transgenic approach might be used to express biosensors in cells in vivo, there is little evidence in the literature that this method will be useful in mammalian models. Transgenic expression of YC2 and camgaroo-2 in *Caenorhabditis elegans* and *Drosophila* neurons, respectively, has been reported ***(32,33)***.
5. All solutions, including KRB and KRH buffers, should be freshly prepared on the same day as the imaging experiments. We strongly recommend avoiding direct application of drugs or other reagents into the specimen chamber by micropipetting; this method does not allow precise control of drug concentration and risks mechanical disruption of cells, which can affect Ca^{2+} signaling. Other methods are available for drug or reagent delivery to cells, including microelectrodes attached to a pressurized microspritzer device or a gravity-fed U-tube connected to a computer-controlled manifold, which receives fluid input from one or more reservoirs. These

methods have the advantage of allowing the administration of reagents to highly localized regions or to individual cells and are especially useful when administering drugs that are available in limited amounts.

6. Under no circumstances should you expose the cells (or your eyes) to unattenuated arc lamp light. Doing so risks photobleaching of the indicator and cell photodamage. Make certain that the digital camera gain is not activated before diverting the emission light path from the binocular eyepieces to the camera. Also, turn off room lights and the condenser lamp before activating the camera. Unfortunately, some intensified digital cameras have limited protection circuitry to prevent damage to the intensifier caused by a sudden exposure to bright light. Apart from outright failure, strong light also greatly decreases the life of Gen-3 intensifiers or can "burn-in" patterns.
7. For Fura-2 imaging using the intensified video camera, we adjust the camera gain using the 380-nm image by initially increasing the camera gain to near saturation, then setting the final adjustment 20–30% below saturation. This is important because as $[Ca^{2+}]$ increases and the 380-nm signal decreases, but as the $[Ca^{2+}]$ returns to baseline or overshoots baseline (which can occur in some Ca^{2+} signaling responses), the 380-nm intensity increases. Setting the camera gain to saturation reduces image quality and impairs reliable quantification of the imaging intensity data. Using the CCD cameras, the 340-nm and 380-nm image gains can be set independently.
8. Use laser power setting of 3–10%, although up to 30% can be required depending on the quality of dye loading. Because emission intensity of Fluo-3 is higher than Fura red, gain settings for the red channel (Fura red) will be higher than the green channel (Fluo-3). As a general rule, we set the gain so that cell fluorescence intensity was at least fivefold above background. The optimal pinhole size, determined by objective numerical aperture (NA) and wavelength, should ideally have different diameters, but many systems have only one pinhole. For live cell work, one must typically open the pinhole wide enough to get adequate signal intensity while keeping the laser intensity low to prevent photobleaching and phototoxicity.
9. Targeted Ca^{2+} biosensors seem to offer an advantage in compartment selectivity; however, compartment physical characteristics, low expression levels, general phototoxicity, and perhaps chaperone content might still seriously hamper measurements. Cameleon probes are not well suited for CLSM using the 488-nm laser because CFP is poorly excited and YFP is directly excited. Some Ar lasers provide a 457-nm line that has been used to excite cameleon probes; however, this line is typically very weak and directly excited YFP. Recent utilization of 405-nm diode lasers in some confocal systems permits strong excitation of CFP with minimal YFP excitation and offers promise that targeted cameleon probes will become more widely used for confocal measurements of compartmental Ca^{2+} fluxes in single cells, tissue slices, or multicellular preparations.

Acknowledgments

This work was supported by an American Diabetes Association Research Award (MWR), NIH DK64162 (MWR), and NIH DK63493 (LHP and MWR).

References

1. Grynkiewicz, G., Poenie, M., and Tsien, R. Y. (1985) A new generation of Ca^{2+} indicators with greatly improved fluorescence properties. *J. Biol. Chem.* **260,** 3440–3450.
2. Kao, J. P. Y., Harootunian, A. T., and Tsien, R. Y. (1989) Photochemically generated cytosolic calcium pulses and their detection by fluo-3. *J. Biol. Chem.* **264,** 8179–8184.
3. Minta, A., Kao, J. P. Y., and Tsien, R. Y. (1989) Fluorescent indicators for cytosolic calcium based on rhodamine and fluorescein chromophores. *J. Biol. Chem.* **264,** 8171–8178.
4. Tsien, R. Y. (1981) A non-disruptive technique for loading calcium buffers and indicators into cells. *Nature* **290,** 527–528.
5. Tsien, R. Y., Pozzan, T., and Rink, T. G. (1982) Calcium homeostasis in intact lymphocytes: cytoplasmic free calcium monitored with a new, intracellularly trapped fluorescent indicator. *J. Cell Biol.* **94,** 325–334.
6. Roe, M. W., Lemasters, J. J., and Herman, B. (1990) Assessment of Fura-2 for measurements of cytosolic free calcium. *Cell Calcium* **11,** 63–73.
7. Takahashi, A., Camacho, P., Lechleiter, J. D., and Herman, B. (1999) Measurement of intracellular calcium. *Physiol. Rev.* **79,** 1089–1125.
8. Baubet, V., Le Mouellic, H., Campbell, A. K., Lucas-Meunier, E., Fossier, P., and Brulet, P. (2000) Chimeric green fluorescent protein-aequorin as bioluminescent Ca^{2+} reporters at the single-cell level. *Proc. Natl. Acad. Sci. USA* **97,** 7260–7265.
9. Miyawaki, A., Llopis, J., Heim, R., et al. (1997) Fluorescent indicators for Ca^{2+} based on green fluorescent proteins and calmodulin. *Nature* **388,** 882–887.
10. Rizzuto, R., Simpson, A. W., Brini, M., and Pozzan, T. (1992) Rapid changes of mitochondrial Ca^{2+} revealed by specifically targeted recombinant aequorin. *Nature* **358,** 325–327.
11. Emmanouilidou, E., Teschemacher, A. G., Pouli, A. E., Nicholls, L. I., Seward, E. P., and Rutter, G. A. (1999) Imaging Ca^{2+} concentration changes at the secretory vesicle surface with a recombinant targeted cameleon. *Curr. Biol.* **9,** 915–918.
12. Foyouzi-Youssefi, R., Arnaudeau, S., Borner, C., et al. (2000) Bcl-2 decreases the free Ca^{2+} concentration within the endoplasmic reticulum. *Proc. Natl. Acad. Sci. USA* **97,** 5723–5728.
13. Griesbeck, O., Baird, G. S., Campbell, R. E., Zacharias, D. A., and Tsien, R. Y. (2001) Reducing the environmental sensitivity of yellow fluorescent protein: mechanisms and applications. *Proc. Natl. Acad. Sci. USA* **276,** 29,188–29,194.
14. Isshiki, M., Ying, Y. -S., Fujita, T., and Anderson, R. G. W. (2002) A molecular sensor detects signal transduction from caveolae in living cells. *J. Biol. Chem.* **277,** 43,389–43,398.
15. Miyawaki, A., Griesbeck, O., Heim, R., and Tsien, R. Y. (1999) Dynamic and quantitative Ca^{2+} measurements using improved cameleons. *Proc. Natl. Acad. Sci. USA* **96,** 2135–2140.

16. Miyawaki, A., Mizuno, H., Llopis, J., Tsien, R. Y., and Jalink, K. (2001) Cameleons as cytosolic and intra-organellar calcium probes, in *Calcium Signalling*, 2nd ed. (Tepikin, A.V., ed.), Oxford University Press, Oxford, pp. 3–16.
17. Mizuno, H., Sawano, A., Eli, P., Hama, H., and Miyawaki, A. (2001) Red fluorescent protein from *Discosoma* as a fusion tag and pardner for fluorescence energy transfer. *Biochemistry* **40,** 2502–2510.
18. Nagai, T., Sawano, A., Park, E. S., and Miyawaki, A. (2001) Circularly permuted green fluorescent proteins engineered to sense Ca^{2+}. *Proc. Natl. Acad. Sci. USA* **98,** 3197–3202.
19. Nagai, T., Ibata, K., Park, E. S., Kubota, M., Mikoshiba, K., and Miyawaki, A. (2002) A variant of yellow fluorescent protein with fast and efficient maturation for cell-biological applications. *Nature Biotechnol.* **20,** 87–90
20. Nakai, J., Ohkura, M., and Imoto, K. (2001) A high signal-to-noise Ca^{2+} probe composed of a single green fluorescent protein. *Nat. Biotechnol.* **19,** 137–141.
21. Pinton, P., Tsuboi, T., Ainscow, E. K., Pozzan, T., Rizzuto, R., and Rutter, G. A. (2002) Dynamics of glucose-induced membrane recruitment of protein kinase C βII in living pancreatic islet β-cells. *J. Biol. Chem.* **277,** 37,702–37,710.
22. Truong, K., Sawano, A., Mizuno, H., et al. (2001) FRET-based *in vivo* Ca^{2+} imaging by a new calmodulin-GFP fusion molecule. *Nature Struct. Biol.* **8,** 1069–1073.
23: Zhang, J., Campbell, R. E., Ting, A. Y., and Tsien, R. Y. (2002) Creating new fluorescent probes for cell biology. *Nature Rev. Cell Biol.* **3,** 906–918.
24. Baird, G. S., Zacharias, D. A., and Tsien, R. Y. (1999) Circular permutations and receptor insertion within green fluorescent proteins. *Proc. Natl. Acad. Sci. USA* **96,** 11,241–11,246.
25. Dustin, L. B. (2000) Ratiometric analysis of calcium mobilization. *Clin. Appl. Immunol. Rev.* **1,** 5–15.
26. Hallett, M. B., Hodges, R., Cadman, M., et al. (1999) Techniques for measuring and manipulating free Ca^{2+} in the cytosol and organelles of neutrophils. *J. Immunol. Methods* **232,** 77–88.
27. Thomas, D., Tovey, S. C., Collins, T. J., Bootman, M. D., Berridge, M. J., and Lipp, P. (2000) A comparison of fluorescent Ca^{2+} indicator properties and their use in measuring elementary and global Ca^{2+} signals. *Cell Calcium* **28,** 213–223.
28. Lipp, P. and Niggli, E. (1993) Ratiometric confocal Ca^{2+} measurements with visible wavelength indicators in isolated cardiac myocytes. *Cell Calcium* **14,** 359–372.
29. Lipp, P., Luscher, C., and Niggli, E. (1996) Photolysis of caged compounds characterized by ratiometric confocal microscopy: a new approach to homogeneously control and measure the calcium concentration in cardiac myocytes. *Cell Calcium* **19,** 255–266.
30. Roe, M. W., Moore, A. L., and Lidofsky, S. D. (2001) Purinergic-independent calcium signaling mediates recovery from hepatocellular swelling: implications for volume regulation. *J. Biol. Chem.* **276,** 30,871–30,877.
31. David, G., Talbot, J., and Barrett, E. F. (2003) Quantitative estimate of mitochondrial $[Ca^{2+}]$ in stimulated motor neurons. *Cell Calcium* **33,** 197–206.

32. Kerr, R., Lev-Ram, V., Baird, G., Vincent, P., Tsien, R. Y., and Schafer, W. R. (2000) Optical imaging of calcium transients in neurons and pharyngeal muscle of *C. elegans*. *Neuron* **26,** 583–594.
33. Yu, D., Baird, G. S., Tsien, R. Y., and Davis, R. L. (2003) Detection of calcium transients in *Drosophila* mushroom body neurons with camgaroo reporters. *J. Neurosci.* **23,** 64–72.
34. Arnaudeau, S., Kelley, W. L., Walsh, J. V., Jr., and Demaurex, N. (2001) Mitochondria recycle Ca^{2+} to the endoplasmic reticulum and prevent the depletion of neighboring endoplasmic reticulum regions. *J. Biol. Chem.* **276,** 29,430–29,439.